

# FeederGAN: Synthetic Feeder Generation via Deep Graph Adversarial Nets

Ming Liang, *Student Member, IEEE*, Yao Meng, *Student Member, IEEE*, Jiyu Wang, *Student Member, IEEE*, David Lubkeman, *Fellow, IEEE*, and Ning Lu, *Senior Member, IEEE*

**Abstract**— This paper presents a novel, automated, generative adversarial networks (GAN) based synthetic feeder generation mechanism, abbreviated as FeederGAN. FeederGAN digests real feeder models represented by directed graphs via a deep learning framework powered by GAN and graph convolutional networks (GCN). From power system feeder model input files, device connectivity is mapped to the adjacency matrix while device characteristics such as circuit types (i.e., 3-phase, 2-phase, and 1-phase) and component attributes (e.g., length and current ratings) are mapped to the attribute matrix. Then, Wasserstein distance is used to optimize the GAN and GCN is used to discriminate the generated graph from the actual. A greedy method based on graph theory is developed to reconstruct the feeder from the generated adjacency and attribute matrix. Our results show that the generated feeders resemble the actual feeder in both topology and attributes verified by visual inspection and by empirical statistics obtained from actual distribution feeders.

**Index Terms**—Deep Learning, Distribution System, Generative Adversarial Networks (GAN), Graph Convolutional Networks (GCN), Graph Theory, Synthetic Feeder.

## I. INTRODUCTION

Test systems are widely used by researchers and engineers to test conceptual designs, optimize parameter settings, and validate performance [1-6]. A test system can be either a real feeder model or a generalized, derived, or extended versions of an actual feeder. For example, a number of new test systems can be obtained by varying the network topology, adjusting the placement and parameters of apparatus (e.g., adding new devices, removing old ones, retrofitting, etc.), and changing user patterns in an actual utility feeder model. A realistic test system needs to faithfully reproduce important distribution system behaviors in different operation conditions so that researchers and engineers can benchmark their algorithms and conduct studies on a wide range of operation conditions with less development time, lower testing cost, and zero risk to interrupt actual system operation.

In recent years, the needs for such realistic distribution feeder test systems are increasing drastically because of the integration of distributed energy resources (DERs). To model the uncertainty and variability in DER operation as well as the variations in its operation environment (e.g., changes in topology, variation in model parameters, user patterns, etc.), an ensemble of realistic distribution test feeders are often needed.

However, developing high-fidelity distribution feeder models requires access to utility network models and customer

data, which is a major barrier for the research community to have unrestrictive, unlimited number of customizable, realistic test systems for research and development purpose. Meanwhile, domain experts, such as operation and planning engineers, have conventions to follow and specific design criterions to meet when designing actual engineering systems. Those inherent characteristics are very hard to be captured by researchers even when they can access actual system models.

Since 1991, 10 IEEE test feeders were developed to meet researcher's needs, approximately. In 2009, led by a group of researchers at Pacific Northwest National lab, 24 taxonomy feeders were developed from 575 actual feeders from 17 utilities across the US [3, 7]. At Texas A&M, researchers are focusing on developing synthetic electric grid models that are designed to be statistically and functionally similar with actual electric grids while containing no confidential critical energy infrastructure information [4].

However, so far, there has been very little attempt made towards the manual and static test system design principles, making creating an ensemble of test systems from actual feeder models a daunting task. In recent years, researchers develop a few methods that use street maps to align and generate feeder layouts [9-11]. For example, in [10], Saha et al. use an open source street map tool to create individual synthetic distribution feeders and groups of feeders in an area with the same ZIP code using a small number of input data, while in [11], Domingo et al. use a reference model to generate large-scale radial feeders using street maps as inputs. In [12-13], Birchfield et al. summarize topological and statistical criterion to validate the realism of synthetic feeders. In [14], Schweitzer et al. conduct a two-stage study to generate synthetic feeders where they treat the feeder as a graph with nodes and edges. In the first stage, a thorough analysis is conducted to summarize the topological and physical characteristics where divergence is used to measure the statistical similarity of real and synthetic feeders. In the second stage, summarized statistics of the feeders are used to generate synthetic feeders having similar characteristics with those Netherland feeders. The shortcoming of these approaches is that they are semi-automatic and lack of the intelligence to learn feeder typology or devices attributes from ingesting actual feeder models, making them unsuitable for generating a large amount of realistic, up-to-date test feeders.

In lieu of this, our aim is to develop an end-to-end, machine-learning-based approach for automated, customizable test feeder generation using actual feeder models as inputs. In [15], Kipf et al. propose the graph convolutional networks (GCN) for

This study is funded by North Carolina State University. Ming Liang, Yao Meng, Jiyu Wang, David Lubkeman and Ning Lu are with the Electrical & Computer Engineering Department, Future Renewable Energy Delivery and

Management (FREEDM) Systems Center, North Carolina State University, Raleigh, NC 27606 USA. (e-mails: [mliang3@ncsu.edu](mailto:mliang3@ncsu.edu), [ymeng3@ncsu.edu](mailto:ymeng3@ncsu.edu), [jwang49@ncsu.edu](mailto:jwang49@ncsu.edu), [dlubkem@ncsu.edu](mailto:dlubkem@ncsu.edu), [nlu2@ncsu.edu](mailto:nlu2@ncsu.edu)).

classifying graph data, such as social network and chemical molecules. Based on GCN, many follow-up studies choose to use a generative adversarial networks (GAN) with GCN to generate graph data. For instance, in [16], Fan and Huang use labeled graph in GAN to generate citation graph and protein graph. A recurrent network based model is used in [17] by You et al. to generate synthetic graphs.

Motivated by those approaches, we develop a GAN-based synthetic feeder generation mechanism, abbreviated as FeederGAN. FeederGAN digests real feeder models using a deep learning framework powered by GAN and graph convolutional networks (GCN). From the information provided in the input files of a power system feeder model, we first map the device connectivity to the adjacency matrix, and then map the device characteristics such as circuit types (i.e., 3-phase, 2-phase, and 1-phase) and component attributes (e.g., length and current ratings) to the attribute matrix, making GCN training possible. Wasserstein distance is used to optimize the GAN for discriminating the generated graph from the actual. We also introduce a method for reconstructing feeder topology from the obtained adjacency and attribute matrix based on graph theory.

Our contributions are three-fold. *First*, the topology is learnt from ingesting actual feeder models instead of street maps, making it possible to extract inherent distribution system design features. *Second*, to our best knowledge, we are the first to use a GAN-based end-to-end and plug-to-play model for generating synthetic feeders. *Third*, FeederGAN is scalable and customizable so its user can generate either a whole feeder or substructures of a feeder at user selected scale and size.

## II. GRAPHICAL REPRESENTATION OF A FEEDER

In this section, we introduce two main considerations when converting a power system feeder model to a machine-learning friendly directed graph model and then discuss the problem formulations of the directed graph model.

The *first* consideration is to omit the geometric information and use the length of the feeder line to represent distance. This is because, in power system network models, the electrical distance used for calculating line impedance is of interest instead of the geographical distance. For visualization purpose, a greedy method (introduced in Section VI.D) is developed to calculate pseudo coordinates for each bus. The substation (i.e., the head of a feeder) is placed at the origin (0, 0). Then, coordinates of subsequent buses are calculated one by one based on electrical distance and connectivity so that the generated synthetic feeder stretches forward as straight as possible, making it easy to traverse feeder topology and identify the relationships between feeder components. As shown in Fig. 1, this approach removes the need for using sensitive customer geographic information, such as street maps and geographic coordinates. From the machine learning standpoint, masking geographical information forces the algorithm to use only the relative distance between line segments, preventing the algorithm from learning from non-generic, geographic information.

The *second* consideration is to replace the traditional bus-as-node and device-as-edge feeder topology representation with a device-as-node representation. Using the device-as-node approach, each device (e.g., a line segment instead of a bus) is defined as a node so the edge will only serve as an indicator to

show the direction pointing from the feeder head to a load node. By doing so, the device attributes, such as length, current ratings, phase, can be defined as node attributes.

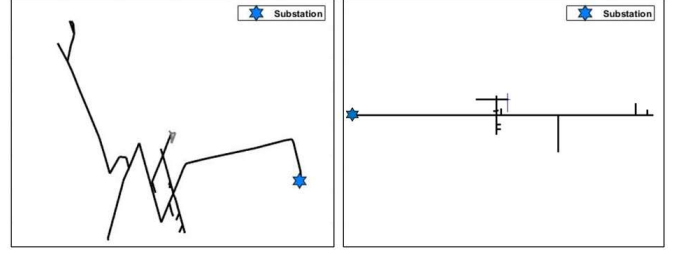


Fig. 1 Topology representation: feeder using geographical coordinates (left) and using electrical distance (right)

The device-as-node representation allows us to represent each device by a node  $v_i \in \mathcal{V}$  and a node attribute vector  $\mathbf{x}_i$ . The feeder can be represented as a directed graph  $\mathcal{G}$  with a set of nodes  $\mathcal{V}$  and edges  $\mathcal{E}$  so that each edge  $(v_i, v_j) \in \mathcal{E}$  connects two nodes and shows the graph direction. Then, the feeder topology can be represented by a directed graph by an adjacency matrix  $\mathbf{A} \in \mathbb{R}^{m \times m}$  and an attribute matrix  $\mathbf{X} = [\mathbf{x}_1, \dots, \mathbf{x}_m]^T \in \mathbb{R}^{m \times d}$ , where  $m$  is the number of nodes,  $A_{ij} \in \{0, 1\}$  and  $d$  is the dimension of the attributes. After converting the feeder topology to a directed graph, the learning algorithm only needs to learn from  $\mathbf{A}$  and  $\mathbf{X}$ , significantly reducing the problem complexity, as shown in Fig. 2.

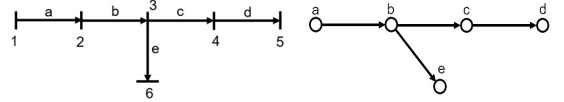


Fig. 2 Distribution feeder topology representation: Bus-as-node and device-as-edge (left) and device-as-node (right)

**Assumption 1:** Because traditional distribution feeders are designed as radial networks, we assume that the feeder graph is a directed radial graph and there is no loop in the graph.

**Property 1:** If Assumption 1 holds, the in-degree is 1 for all nodes except the feeder head node, whose in-degree is 0. This property suggests that there should be one and only one non-zero element in each column of the adjacency matrix  $\mathbf{A}$ , except for the column representing the feeder head.

Once a feeder model is converted to  $\mathbf{A}$  and  $\mathbf{X}$ , we can use a GAN-based framework to learn from the real feeder and generate the topology  $\hat{\mathbf{A}}$  and attributes  $\hat{\mathbf{X}}$  for a synthetic feeder.

## III. PROBLEM FORMULATION

This section introduces the deep learning concepts used in the paper, the preparation of training data, and the problem formulation of GAN and GCN for generating synthetic feeder topology and attributes.

### A. An Introduction of the Deep Learning Framework

FeederGAN digests real feeder models using a deep learning framework powered by GAN and GCN. Deep learning refers to deep neural networks built on several layers of neurons. If the layer is linearly and fully connected, it is called a fully connected (FC) layer. A model built on several FC layers is called multilayer perceptron (MLP). To model the non-linearity in the dataset, activation functions are used. In this paper, two major activation functions are rectified linear units (ReLU) and softmax. ReLU [18] is formulated as  $f(x) = \eta x$ ,

where  $\eta = 1$  when  $x > 0$ ;  $\eta = 0$  when  $x \leq 0$ . If the negative part  $\eta$  is a small but non-zero value, the method is called leaky ReLU [18]. Softmax [19] is formulated as  $f(x_i) = e^{x_i} / \sum_j e^{x_j}$ . Softmax is often used in classification or approximating discrete one-hot values, where a discrete variable is encoded as a vector consisting of binary values (i.e., 0/1). When using Softmax, the output of each layer is normalized as a probability and the sum of all outputs is one.

### 1) Generative Adversarial Networks (GAN)

As shown in Fig. 3, a GAN [20] consists of two main components: Generator and Discriminator. Discriminator distinguishes whether the input data is real or fake (i.e., generated) while Generator generates fake data sets resembling the real data to exploit weakness in Discriminator. Thus, GAN learns to generate high-quality fake data sets by letting Generator and Discriminator play a minimax game, which ends when Discriminator can no longer distinguish the generated and real data. This process can be formulated as

$$\min_G \max_D V = \mathbb{E}_x[\log(D(x))] + \mathbb{E}_z[\log(1 - D(G(z)))] \quad (1)$$

where  $D(x)$  is Discriminator outputs,  $G(z)$  represents Generator output,  $x$  represents the real data, and  $z$  represents a random noise. For Discriminator, the first part of (1) is to predict the real as real, and the second part is to predict the fake as fake.  $D(x)$  outputs are interpreted as probability with 1 for real and 0 for fake. To make the Discriminator output a probability, a sigmoid function [20] is added to the Discriminator output layer to normalize  $D(x)$  into  $[0, 1]$ . For Generator, the first part of (1) is not used because the Generator goal is to make Discriminator “think” the fake is real.

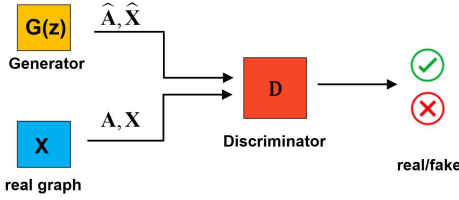


Fig. 3 Framework of a typical GAN

### 2) Graph Convolutional Networks (GCN)

GCN [15] uses the adjacency matrix  $\mathbf{A}$  to represent the connectivity between nodes and the attribute matrix  $\mathbf{X}$  to store nodal device information. The GCN representation of a directed graph is

$$\bar{\mathbf{A}} = \mathbf{D}^{-1}(\mathbf{A} + \mathbf{I}) \quad (2)$$

$$\text{GCN}(\bar{\mathbf{A}}, \mathbf{X}) = \sigma(\bar{\mathbf{A}}\mathbf{X}\mathbf{W}) \quad (3)$$

where  $\mathbf{I}$  is an identity matrix,  $\mathbf{D}$  is a diagonal degree matrix with  $\mathbf{D}_{ii} = 1 + \sum_j \mathbf{A}_{ij}$ , and  $\mathbf{W}$  is the network parameter matrix to be learnt.  $\sigma(\cdot)$  is an activation function (e.g., ReLU). Note that by using (2), a row-wise normalization is executed to  $\mathbf{A}$ . To simplify future derivations, we let  $\mathbf{A}$  be the normalized adjacency matrix in the rest of the paper.

### B. Feature Engineering

Feeder topology information, i.e., the connectivity between feeder nodes, are coded into  $\mathbf{A}$ , a  $m \times m$  matrix. Let  $\mathbf{A}_{i,j} = 1$  if there is a connection from node  $i$  to  $j$  (unilateral) and let  $\mathbf{A}_{i,j} = 0$  otherwise. After the whole network is traversed, use (2) to normalize  $\mathbf{A}$ .

As shown in Table I, there are two types of features in  $\mathbf{X}$ : organic and topological. Organic features include device length, current rating, and phase, the information of which can be directly extracted from device definition files. Topological features include the distance between the device and the feeder head, pseudo loads the device carries, and the device level in the overall feeder topology hierarchy. Topological features are obtained by traversing the feeder topology using either the depth-first search (DFS) or the breadth-first search (BFS).

In Table I, the first four features have continuous, numerical values and are normalized by their extreme values to uniformly map them into  $[-1, 1]$ ; the last two features are categorical features that bear discrete values and are encoded by one-hot values. Thus, numerical attributes are represented by  $\mathbf{X}_{num} \in \mathbb{R}^{m \times 4}$  and categorical attributes by  $\mathbf{X}_{cat} = [\mathbf{X}_{cat}^1, \mathbf{X}_{cat}^2] \in \mathbb{R}^{m \times (d_1 + d_2)}$ , where  $m$  is the number of nodes, and  $d_1, d_2$  are the dimension of each categorical feature, i.e., the number of categories for each feature.

Table I A summary of the attributes  
O: organic, T: topological, N: numerical, C: categorical

Name	Definition	Type	Source
Length	The length of a device.	N	O
Norm Amps	Normal condition conductor amps, an indicator for the conductor materials.	N	O
Distance	Distance from feeder head to the device.	N	T
Pseudo Load	The sum of the capacity of all downstream customer side transformers.	N	T
Level	Start as Level 0 at the feeder head. When encountered a bifurcation leading to several children branches, level+1 if “norm amps” or “phase” of the child is different from that of the parent.	C	T
Phase	1 of the 7 options: $a, b, c, ab, ac, bc, abc$	C	O

### C. FeederGAN Algorithm and Training Strategy

In our experiments, the minimax GAN problem formulated in (1) suffers convergence issues caused by gradient vanishing, where the loss of Discriminator decreases quickly when reaching to an optimal solution, causing backward gradients of the Generator to drop to 0. As a result, the Generator can no longer be trained properly. To solve this problem, we apply the Wasserstein GAN (WGAN) introduced by Arjovsky in [21]. WGAN shares the same model structure with GAN, but by removing the sigmoid output layer of the GAN, WGAN directly outputs a logit, called the critic score, instead of a probability. Thus, the gap of the critic score between a real graph and a generated graph, called the Wasserstein distance, can be used to train the Generator and Discriminator.

The WGAN formulation is

$$\min_G \max_D V = \mathbb{E}_x[D(x)] - \mathbb{E}_z[D(G(z))] \quad (4)$$

where  $x$  is the real graph, i.e.  $\{\mathbf{A}, \mathbf{X}_{num}, \mathbf{X}_{cat}\}$ ,  $z$  is a random noise matrix, and  $G(z)$  is the generated graph  $\{\hat{\mathbf{A}}, \hat{\mathbf{X}}_{num}, \hat{\mathbf{X}}_{cat}\}$ ,  $\mathbb{E}_x[D(x)]$  and  $\mathbb{E}_z[D(G(z))]$  is the critic score the Discriminator gives to the real graph and the generated graph, respectively. Now, the Discriminator’s objective is to widen the Wasserstein distance while the Generator’s objective is to narrow it.

When there is no constraint on the Discriminator, the value of the Discriminator weights will gradually grow larger and larger and thus fail to train Generator properly. Hence, the Discriminator will be subject to a constraint called the  $k$ -Lipschitz condition such that

$$|D(x_1) - D(x_2)| < k \times |x_1 - x_2| \quad (5)$$

To implement the Lipschitz condition, we conduct weights clipping so that the weights of Discriminator are clamped within  $(-c, c)$ , where  $c$  is the clipping limit. The FeederGAN algorithm is summarized in Algorithm 1.

**Algorithm 1.** FeederGAN. All experiments in the paper used the default training parameters  $\alpha=0.0001$ ,  $c=0.1$ ,  $n=20$ ,  $n_0=500$ ,  $n_1=1000$ ,  $n_2=5$ .

**Require:**  $\alpha$ , the learning rate;  $c$ , the weight clipping limit;  $n_1$ ,  $n_2$ , the number of iterations for Discriminator at different stages;  $n$ ,  $n_0$ , the numbers separate different training stages;  $\omega_0$ , initial Discriminator parameters;  $\theta_0$ , initial Generator parameters.

```

1:  $i = 0$ 
2: while  $\theta$  not converge do
3:    $iter \leftarrow n_1$ , if  $i < n$  or  $i \% n_0 = 0$ 
4:    $iter \leftarrow n_2$ , else
5:   for  $t=1, 2, \dots, iter$  do
6:     Draw a sample  $\{A, X_{num}, X_{cat}\}$  from the real dataset
7:     Generate a random matrix  $z$  from the prior distribution
8:      $\{\hat{A}, \hat{X}_{num}, \hat{X}_{cat}\}_\theta \leftarrow G_\theta(z)$ 
9:      $g_\omega \leftarrow \nabla_\omega [D_\omega(\{A, X_{num}, X_{cat}\}) - D_\omega(\{\hat{A}, \hat{X}_{num}, \hat{X}_{cat}\}_\theta)]$  (6)
10:     $\omega \leftarrow \omega + \alpha \cdot \text{RMSProp}(\omega, g_\omega)$ 
11:     $\omega \leftarrow \text{clipping}(\omega) - c, c$ 
12:  end for
13:  Generate a random matrix  $z$  from prior distribution
14:   $\{\hat{A}, \hat{X}_{num}, \hat{X}_{cat}\}_\theta \leftarrow G_\theta(z)$ 
15:   $g_\theta \leftarrow -\nabla_\theta [D_\omega(\{\hat{A}, \hat{X}_{num}, \hat{X}_{cat}\}_\theta)]$  (7)
16:   $\theta \leftarrow \theta - \alpha \cdot \text{RMSProp}(\theta, g_\theta)$ 
17:   $i \leftarrow i + 1$ 
18: end while

```

Lines 3-4 illustrate the strategy used to train Discriminator as strong as possible. As shown in Fig. 4, in the first few iterations, the Generator will be trained once every  $n_1$  Discriminator training cycles. After the Generator has been trained  $n$  times, the frequency will be reduced to train Generator once every  $n_2$  Discriminator training cycles. Then, at the  $n_0, 2n_0, 3n_0, \dots$  Generator training cycles, we will enforce an aggressive training snapshot to train the Discriminator  $n_1$  times, before training the Generator. By doing so, we can train the Discriminator as strong as possible to widen the Wasserstein distance, making it easy to distinguish the real graph from the generated ones. If the Generator can be trained to narrow the Wasserstein distance, the generated graphs eventually will be realistic enough to cheat the Discriminator.

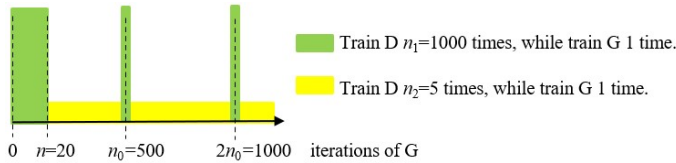


Fig. 4. FeederGAN training schedule

Lines 5-12 illustrate the Discriminator training process. At each training session, a real graph combined with a generated graph are used to obtain the Wasserstein distance. Then, we fix the parameters of the Generator and trace backward to calculate the gradients using (6). After that, we use the RMSProp algorithm [22] to adaptively update the weights of the Discriminator. In the end, we conduct a weight clipping so that for weights smaller than  $-c$ , set them at  $-c$ ; for weights larger than  $c$ , set them at  $c$ . Similarly, lines 13-16 describe how to calculate the Generator gradients and update its weights.

## IV. FEEDERGAN IMPLEMENTATION

This section introduces the architecture of the Generator and the Discriminator as well as hyperparameters.

### A. Generator Architecture

As shown in Fig. 5, a multilayer perceptron (MLP) that has several FC layers is used to generate  $\hat{A}$  and  $\hat{X}$ . The random noise matrix  $Z$  is generated using a prior Gaussian distribution and the latent matrix  $L$  is generated using FC1. FC2 is used to generate the numerical attributes  $\hat{X}_{num}$  and a hyper tangent activation function is used to scale  $\hat{X}_{num}$  within  $[-1, 1]$ , the same value range as the real attributes. The process is described as

$$L = \text{FC1}(Z), \hat{X}_{num} = \text{FC2}(L), \hat{X}_{num} = \tanh(\hat{X}_{num}). \quad (8)$$

To generate the categorical features, we first use FC3 to generate  $V$ , the latent matrix for all categorical features. Then, a separate FC4- $i$  layer is used to generate the  $i^{\text{th}}$  categorical feature. After that, a row-wise softmax activation function is used to approximate the one-hot encoded categorical feature before outputting it to  $\hat{X}_{cat}^i$ . The use of *softmax* makes the network differentiable. Note that if a hard encoding method that is not non-differentiable (e.g., *argmax*) is used, the gradient backward pass will be broken. This process for generating the categorical features is described as

$$V = \text{FC3}(L), \hat{X}_{cat}^i = \text{FC4} - i(V), \hat{X}_{cat}^i = \text{softmax}(\hat{X}_{cat}^i) \quad (9)$$

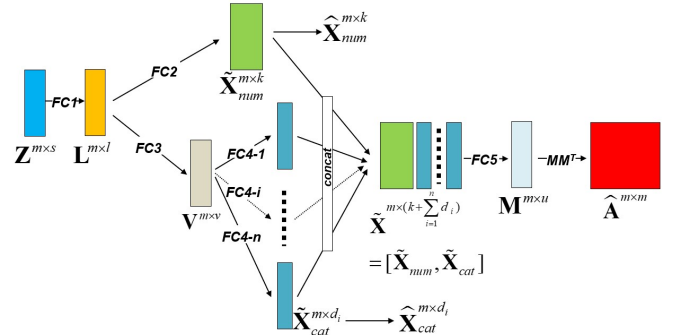


Fig. 5. Generator architecture

The numerical and categorical features (before activation) are then concatenated to form the latent matrix  $\tilde{X}$ . Since the two features have different value scales, they will first be normalized then go through FC5 to generate  $M$ .  $M$  is then multiplied by its transpose to form an  $m \times m$  matrix, which will then go through a column wise softmax activation function to obtain  $\hat{A}$ . Using column-wise softmax, we can map all  $\hat{A}$  entries to  $[0, 1]$  while enforcing Property 1 (i.e., only 1 non-zero entity in each column), making those potentially non-zero entities stand out. This process is formulated as

$$\tilde{X} = \text{norm}([\tilde{X}_{num}, \tilde{X}_{cat}]), M = \text{FC5}(\tilde{X}), \hat{A} = \text{softmax}(M \times M^T) \quad (10)$$

### B. Discriminator Architecture

The objective of the Discriminator is to distinguish the real and generated graphs. The discriminative process for both the real and the generated graphs is the same, as shown in Fig. 6. Hence, only the generated set of data  $\hat{A}$ ,  $\hat{X}_{num}$ ,  $\hat{X}_{cat}$  are used to illustrate the discriminative process.

Categorical features are either one-hot encoded or softmax approximated, so an embedding layer *emb- $i$*  is used to project those discrete values into a lower dimension matrix,  $P_i$ . Thus,



the embedding process not only conducts dimension reduction, but also maps the discrete, sparse values into continuous, dense values, making it possible for the categorical features to be processed together with the numerical features.

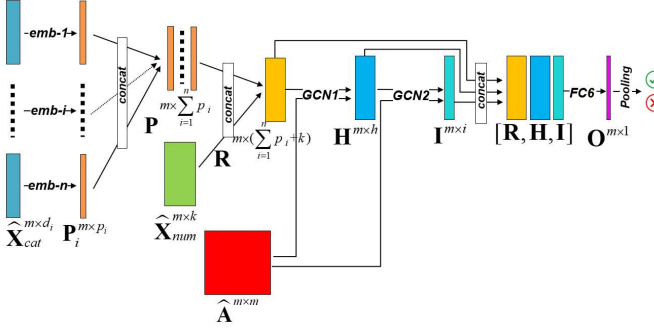


Fig. 6. Discriminator architecture

Symmetrically as in the generative process, all the embedding results are concatenated as a latent representation  $\mathbf{P}$ , for categorical features. Then,  $\mathbf{P}$  is concatenated with the numerical features and go through a layer normalization to get the latent matrix  $\mathbf{R}$  for all the attributes. The attributes processing is formulated as

$$\mathbf{P}_i = \text{emb} - i(\hat{\mathbf{X}}_{cat}^i), \mathbf{R} = \text{norm}([\mathbf{P}, \hat{\mathbf{X}}_{num}]) \quad (11)$$

Next, we use the adjacency matrix to filter the attributes via two GCN layers. Since GCN is prone to gradient vanishing problem, a residual structure is used to aggregate the latent matrices  $\mathbf{R}, \mathbf{H}, \mathbf{I}$  together. Hence, the gradient backward pass becomes a three-way pass instead of a single one to boost the gradients back and benefit the training of the Generator.

In the second to the last layer, FC6 processes the concatenated residual matrices to obtain a vector  $\mathbf{O}$  with  $m$  entities that reveals the latent information for each node. Finally, a global pooling method, e.g. max-pooling, is used to output a single value serving as the critic score. The discriminative process is formulated as

$$\mathbf{H} = \text{GCN1}(\hat{\mathbf{A}}, \mathbf{R}), \mathbf{I} = \text{GCN2}(\hat{\mathbf{A}}, \mathbf{H}) \quad (12)$$

$$\mathbf{O} = \text{FC6}([\mathbf{R}, \mathbf{H}, \mathbf{I}]), \text{score} = \text{pooling}(\mathbf{O}) \quad (13)$$

Note that besides softmax and hyper tangent, we use ReLU after certain FC layers and leaky ReLU after GCN to introduce non-linearity.

### C. Hyperparameters

The major hyperparameters are listed in the first row of Algorithm 1. To guarantee the convergence of Wasserstein distance, experiments need to be conducted to tune the learning rate. In our paper, we choose a learning rate  $\alpha=0.0001$ . The clipping limit  $c$  is also determined through experiments and is set at 0.1 to avoid gradient vanishing and exploding.

The dimension of the random noise matrix  $\mathbf{Z}$  is  $m \times s$ , where  $m$  is the number of nodes that is adaptive to the real graphs;  $s$  is the parameter to be tuned, and we set as 20 in this paper. The size of the hidden layers is subject to the size of the real graphs where typical values of 128 and 64 are used.

### V. FEEDER RECONSTRUCTION

Once the training of Generator finished, we can use it to generate  $\hat{\mathbf{A}}$  and the attributes matrix  $\hat{\mathbf{X}}_{num}, \hat{\mathbf{X}}_{cat}$ , which are either softmax-approximated to be within  $[0, 1]$  or hyper

tangent approximated to be within  $[-1, 1]$ . Then, we use the reconstruction methods to map them back to the actual values.

#### A. Reconstruction of the Adjacency Matrix

The entities in the generated adjacency matrix  $\hat{\mathbf{A}}$  have continuous values in  $[0, 1]$ . Algorithm 2 is used to reconstruct the binary directed adjacency matrix for the feeder from  $\hat{\mathbf{A}}$ .

##### Algorithm 2. Adjacency Matrix Reconstruction.

**Require:**  $\hat{\mathbf{A}}$ , the generated soft adjacency matrix; *row*, the number of rows in the adjacency matrix; *col*, the number of columns in the adjacency matrix.

```

1: for  $i=1, 2, \dots, \text{row}$  do
2:   for  $j=i, i+1, \dots, \text{col}$  do
3:      $\hat{\mathbf{A}}_{j,i} \leftarrow 0$ , if  $\hat{\mathbf{A}}_{i,j} \geq \hat{\mathbf{A}}_{j,i}$ 
4:      $\hat{\mathbf{A}}_{i,j} \leftarrow 0$ , if  $\hat{\mathbf{A}}_{i,j} < \hat{\mathbf{A}}_{j,i}$ 
5:   end for
6: end for
7:  $\tilde{\mathbf{A}} \leftarrow \hat{\mathbf{D}}^{-1} \hat{\mathbf{A}}$ 
8: for  $j=1, 2, \dots, \text{col}$  do
9:    $k \leftarrow \text{argmax}(\tilde{\mathbf{A}}_{:,j})$ ,  $\tilde{\mathbf{A}}_{k,j} \leftarrow 1$ 
10:  for  $i=1, \dots, \text{row}$  and  $i \neq k$  do
11:     $\tilde{\mathbf{A}}_{i,j} \leftarrow 0$ 
12:  end for
13: end for
14: return  $\tilde{\mathbf{A}}$ 

```

In lines 1-6, to make a directed graph out of  $\hat{\mathbf{A}}$ , for any symmetrical pair  $\hat{\mathbf{A}}_{ij}$  and  $\hat{\mathbf{A}}_{ji}$ , there should be one non-zero entity at most. Hence, we set the smaller one as 0 and keep the larger one as it is. In line 7, we conduct a row-wise normalization, which is also used in the feature engineering process as an import procedure to guarantee sparsity. In lines 8-13, we conduct Property 1, i.e. in each column we set the largest entity as 1 and the rest as 0. After that,  $\tilde{\mathbf{A}}$  becomes a binary, sparse adjacency matrix describing a directed graph.

#### B. Topology Reconstruction

In graph theory, node ordering can be problematic, because for a specific adjacency matrix, the different ordering of nodes can represent different topologies. For the Discriminator, because GCN is ordering invariant, node ordering is not an issue. However, for Generator, MLP is ordering variant, so node ordering needs to be addressed. Note that using permutation to resolve the node ordering is impossible as a graph with  $m$  nodes has  $m$ -factorial ( $m!$ ) possibilities.

To reduce the complexity, one can permute only the position of the feeder head based on the reconstructed  $\tilde{\mathbf{A}}$ , which has only 1 non-zero entity in each column. The algorithm is illustrated in Algorithm 3. The node-to-edge transformation (in line 5) is an inverse procedure of Fig. 2. Therefore, for each generated adjacency matrix, theoretically,  $m$  topologies can be obtained at the most. For more detailed explanations, please refer to Example 1 in Appendix.

##### Algorithm 3. Feeder Head Permutation.

**Require:**  $\tilde{\mathbf{A}}$ , the reconstructed binary directed matrix;  $m$ , the node number.

```

1: for  $i = 1, 2, \dots, m$  do
2:   if row  $i$  with non-zero entities do
3:     Set the corresponding column  $i$  as all 0s;
4:     Let node  $i$  be the feeder head and traverse the adjacency matrix to build the graph;
5:     Conduct a node-to-edge transformation to build the feeder topology.
6:   end if
7: end for

```

### C. Attributes Reconstruction

After reconstructing the feeder topology, we need to assign attributes to each device so that a distribution feeder model in the targeted format (e.g., OpenDSS, CYME) can be produced. Among all attributes, topological features are just used to facilitate the discriminative inference, which are not necessary to be reconstructed. Hence, we only need to reconstruct the organic features.

For “length”, we map the generated value from  $[-1, 1]$  to  $[0, 800]$  uniformly, where 800 m is the nominal maximum value of a feeder line segment. Note that one can pick a suitable maximum value based on his modeling need. Although the “norm amps” is used as a continuous value, it’s used to represent the conductor material information, e.g. line code, thus the category of the values is limited to about 10. Hence, based on the generated value, we use a lookup table for line codes to assign the nearest “norm amps” value. Among all attributes, “phase” is the most important one because it affects how realistic a generated feeder is. As *softmax* is used to approximate the one-hot encoding, an *argmax* function is used to map the phase type to the 7 choices.

### D. Visualize the Generated Feeder

As the geometric coordinates have been omitted in the learning process, we need to generate pseudo coordinates for each bus to plot out the feeder topology for inspection. A greedy method (as described in Algorithm 4) is developed to generate the pseudo coordinates with two objectives: making the feeder lines as straight as possible while reducing the chance of overlapping and crossing. For more details, please refer to Example 2 in Appendix.

---

#### Algorithm 4. Feeder Topology Visualization

---

- 1: Set the feeder head as the origin (0,0) and traverse the rest of the feeder;
  - 2: Set the direction as straight right and make the direction angle as  $\theta = 0$ ;
  - 3: If no bifurcation, keep the current direction, calculate the coordinate of the next bus using the line length;
  - 4: When there is a bifurcation, rank the priority of children branches based on the number of its downward devices. The large the number, the higher the ranking;
  - 5: The 1<sup>st</sup> child branch keeps the same direction as parent’s, the 2<sup>nd</sup> and 3<sup>rd</sup> children’s angle plus a delta angle  $\delta$  ( $\pi/2$ ) and  $(-\pi/2)$  respectively. If there are more children in the branch, use more angles, e.g. ( $\pi/4$ ), ( $3\pi/4$ ), ( $-\pi/4$ ), ( $-3\pi/4$ ), ( $\pi/8$ ), ...;
  - 7: Update the children branch’s direction angle, calculate the corresponding bus coordinates with the angle, the length of the line, and the parents’ coordinates.
- 

## VI. RESULTS AND DISCUSSION

### A. Dataset and Augmentation

We use real feeder models with 1500 to 2000 overhead lines and cables as inputs in this study. First, all tie switches are set as “open” to satisfy Assumption 1 (i.e., no loops). Second, we sample sub-feeder structures from full feeder networks to augment the training database using Algorithm 5. Then, the full feeder network and the sampled sub-feeder structures are used as the training dataset, in which we have 664 graphs in total.

---

#### Algorithm 5. Subgraph Sampling.

---

**Require:** A pool of real feeders served as real graphs

---

- 1: Select a start node from level 0 or level 1 nodes;
  - 2: Extract all its downstream nodes (all the way to loads) to form a subgraph;
  - 3: If number of nodes is less than 100, resample;
  - 4: If the number of nodes is more than 50% of the original graph, resample;
  - 5: Repeat for desired times.
- 

### B. Training Loss and Generated Feeders

In Fig. 7, the training losses of the Discriminator when feeding with real and generated (fake) graphs, and the Wasserstein distance are shown on the left; the zoom-in plots for each training stage are shown on the right. The x-axis is the number of iterations for Generator. Note that one Generator iteration corresponds to multiple Discriminator iterations.

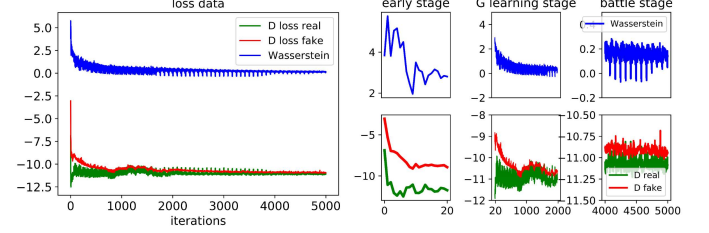


Fig. 7. Loss and Wasserstein distance

In the first few iterations, we train Discriminator to be very strong so it can easily widen the Wasserstein distance. When the training proceeds, although the Discriminator is trained more times than the Generator, the Generator learning process will gradually narrow the Wasserstein distance until the distance converges to a very small but non-zero oscillatory equilibrium, as shown in the zoom-in plots. Meanwhile, the critic score for the real and the fake vibrates around an equilibrium point. It shows that the Generator generates graphs of good quality that the Discriminator can no longer tag them.

Figure 8 shows examples of the feeder topologies generated by the FeederGAN, from which, an expert can examine the feeder layout and exclude the ones that do not meet their requirements. Note that we only generate line segments, i.e., overhead lines or cables in current stage. Reclosers or regulators can be added later based on different modeling needs by the user.

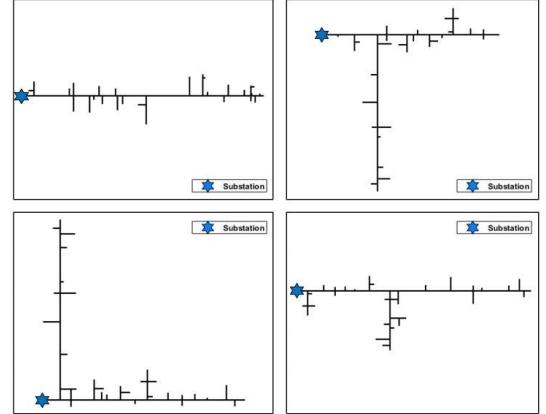


Fig. 8. Generated feeders

### C. Performance, Mode Collapse and Human Guidance

We define 3 performance metrics in Table II to evaluate the generating process. The first metric is to pass a connectivity check. An adjacency matrix is *connected* when the matrix contains fully connected graph without isolated partitions. So an adjacency matrix containing isolated blocks will fail the connectivity check because it causes the generated graph to break into a few disconnected pieces. The second and third metrics are *Success* and *Perfect*, which are related with the continuity of feeder phase transitions. For example, only  $a, b$  or

$ab$  line segments can be branched out from a line segment having the  $ab$  phase attribute.

Table II Definition of the Success and Perfect metrics

Success definition		Perfect definition	
phase	subsequent neighbor's phase	phase	subsequent neighbor's phase
3 phases	3 phases,	$abc$	$abc, ab, ac, bc, a, b, c$
	2 phases,	$ab$	$ab, a, b$
	single phase	$ac$	$ac, a, c$
2 phases	2 phases,	$bc$	$bc, b, c$
	single phase	$a$	$a$
single phase	single phase	$b$	$b$
		$c$	$c$

Recall that there are  $m$  possible topologies for each reconstructed adjacency matrix  $\tilde{A}$  when applying the feeder-head permutation method. So the 3 types of *performance rates* are defined as the ratio of the fully *connected*, *success* and *perfect* generated graphs among all  $m$  options. In training, after every 50 Generator iterations, we output a set of generated graphs and calculate the performance rates. The rates can vary often because they are calculated using the results of a snapshot. Therefore, we average those rates in a 500-iteration window, making each data point represent an average value of 10 results during 500 iterations. As shown in the left plot in Fig. 9, the model performance improves to 25% after 4000 iterations, meaning that 25% of the  $m$  generated feeder topologies are connected, success, and perfect.

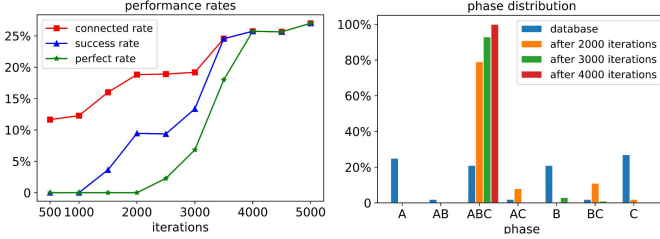


Fig. 9. Performance rates (left) and phase mode collapse (right)

During the training, we observed two major problems related with mode collapse [23], where the Generator locked into one or a few limited modes to exploit the Discriminator. The first is phase mode collapse. As shown in the right plot in Fig. 9, at the beginning of the training, 3-phase and single phase circuits are mixed evenly. However, after 2000 iterations, 3-phase circuits start to dominate with the presence of a small number of 2-phase (i.e.,  $ac$  and  $bc$ ) circuits; while towards the end, all circuits converge to 3-phase. To solve this problem, the early-stop-strategy is used to terminate the training after approximately 3000 to 4000 iterations, when the phases generated are not all 3-phase circuits. Then, we use the human guidance to assign the phase information to line segments as illustrated in Algorithm 6. The advantage of applying human guidance are twofold: achieve a user-defined phase diversity and convert previously imperfect generated circuit topology to a perfect one.

**Algorithm 6.** Human Guidance for Phase Assignment.

- 1: Traverse the feeder from the feeder head with 3-phase attribute, i.e.,  $abc$ ;
- 2: Keep the phase attribute until reaching a bifurcating point;
- 3: Check for possible phase options via perfect definition in Table II;
- 4: Select from the possible choices the one with the highest score in the generated *softmax* approximated phase results, i.e.  $\hat{x}_{cat}^2$ .

The second is topology mode collapse. We have plotted a few graphs to show the topologies of a few generated circuits at different locations in the Wasserstein loss curve, as shown in Fig. 10. At the very beginning, the feeder generated is dense and has shorter backbones. After 2000 iterations, the feeder shows a longer backbone with branches. But after 4000 iterations, the backbone remains but the branches disappear, showing a single line without bifurcation. This problem can be addressed by an early stop. In our experiments, we stop the training after 3000-4000 iterations to get satisfactory results.

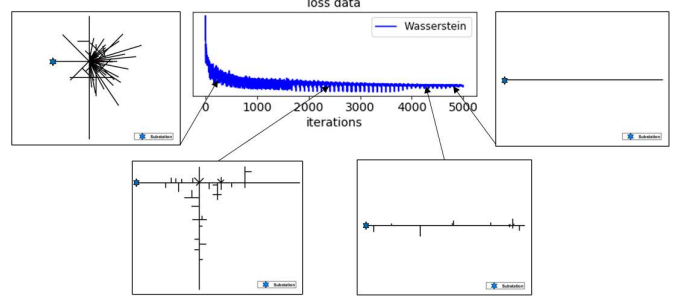


Fig. 10. Topology mode collapse

**D. Quality Evaluation and Empirical Statistics**

When using FeederGAN to generate synthetic feeders, we can generate  $m$  possible candidates each time for a feeder with  $m$  devices via feeder head permutation (Algorithm 3). Then, we use the empirical statistics method for measuring realism, in which the statistical characteristics of real distribution feeder models (See Table III) are compared with those of the generated ones. If the statistics of a generated feeder are outside the empirical range, it will be discarded. The first measurement is “level”, which measures the feeder topology hierarchy from the feeder head to the lowest downward load node. If a generated feeder has more than 10 levels, it is discarded. The second measure is the ratio of 3-phase, 2-phase, and 1-phase circuits because a realistic feeder usually has more 1-phase circuits and 3-phase with only a few being 2-phase. The third measure is the out-degree of a node defining the number of its subsequent neighbors. For a realistic feeder topology, 99% times the out-degree is less than 5. What’s more, if the probability distribution of the length of generated line segments differs a lot from the real one (as shown in Fig. 11), we can either discard it or use the probability distribution of real feeders to conduct a 2<sup>nd</sup> round “length” re-generation, which will make sure that the length of each generated line segment is realistic.

Table III Empirical statistics

metrics	empirical value						
levels	4 ~ 7						
phase distribution	$a$	$ab$	$abc$	$ac$	$b$	$bc$	$c$
	18%~28%	1%~3%	20%~25%	1%~3%	18%~28%	1%~3%	18%~28%
out-degree distribution	0	1	2	3	4	$\geq 5$	
	20%~40%	25%~45%	18%~26%	5%~7%	1%~3%	<1%	

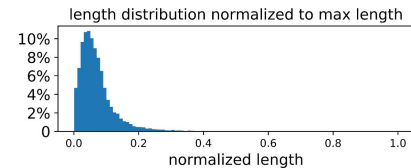


Fig. 11. Probability distribution of the length of the line segments

## VII. CONCLUSION AND FUTURE WORK

In this paper, we introduced FeederGAN, a novel GAN-based method, to enable automated, high fidelity synthetic feeder generation. FeederGAN ingests power system distribution feeder models as directed graphs using a device-as-node representation. Feeder topology and device characteristics are coded into the adjacent matrix and the attribute matrix to allow GCN-based methods to learn topology and attributes from actual power system feeder model input files. This approach will make FeederGAN *expandable* (handling feeders at different scales with any number of customized attributes) and having superb learning flexibility (learning from a full network structure or substructures). To solve the mode collapse problem, *early stop* and *human guidance* are proposed. The realismness of the generated feeder topology can be validated by visual inspection and empirical statistics. Our simulation results have shown that even an expert cannot distinguish the generated topologies from the real ones. By comparing the empirical statistics, the generated synthetic feeders match well with the actual. This research aims at meeting the research needs of researchers for conducting distribution system planning studies and for developing control and energy management algorithms, where a large amount of realistic test feeders are needed. Our future work will focus on automated device placement so that sectionalizers and voltage regulation devices can be automatically added to the feeder model.

## APPENDIX

**Example 1:** This example illustrates the reconstruction process via feeder head permutation. As shown in Fig. A1, the reconstructed  $\tilde{\mathbf{A}}$  has only 1 non-zero entity in each column with only row 1, 2, and 3 has non-zero entities. Hence, nodes 1, 2 and 3 are the candidates for the feeder head node. If node 1 is chosen, set all entities in column 1 as 0. Traverse all the nodes to build the directed graph, i.e.  $1 \rightarrow 2, 2 \rightarrow 3/4/5$ . Then, convert a node-to-edge transformation so a feeder topology is obtained following the power system conventions.

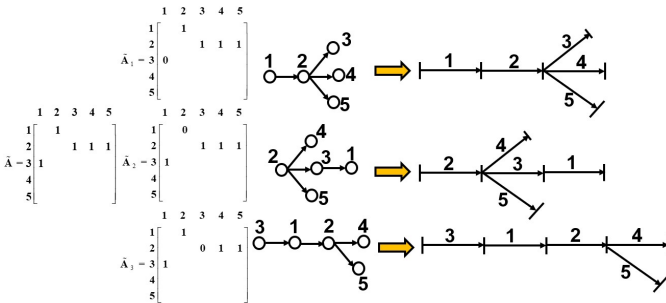


Fig. A1. Topology Reconstruction

**Example 2:** In Fig.A2, we illustrate how to calculate the pseudo coordinates. Suppose we have already traversed to bus  $j$  with a coordinate at  $(x_j, y_j)$  and a branch direction of  $\theta$ . The bifurcation leads to 4 children branches. The device linking bus  $j$  and  $k$  with fewest downward devices will have the lowest priority ranking with an angle assigned as  $\delta$ . Hence, for this branch, the direction angle is updated as  $\theta + \delta$ . The coordinate of bus  $k$  is  $(x_k, y_k)$ , calculated by  $x_k = x_j + l \cdot \cos(\theta + \delta)$ ,  $y_k = y_j + l \cdot \sin(\theta + \delta)$ , where  $l$  is the device length between bus  $j$  and  $k$ .

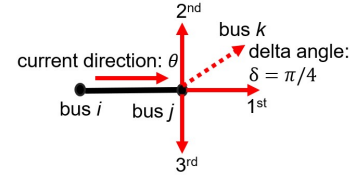


Fig. A2. Pseudo Coordinates calculation

## REFERENCES

- [1] W. H. Kersting, "Radial distribution test feeders," in *2001 IEEE Power Engineering Society Winter Meeting. Conference Proceedings (Cat. No. 01CH37194)*, 2001, vol. 2, pp. 908–912 vol.2.
- [2] "PES Test Feeder." [Online]. Available: <https://site.ieee.org/pes-testfeeders/resources/>.
- [3] "Feeder Taxonomy - GridLAB-D Wiki." [Online]. Available: [http://gridlab-d.shoutwiki.com/wiki/Feeder\\_Taxonomy](http://gridlab-d.shoutwiki.com/wiki/Feeder_Taxonomy).
- [4] "Electric Grid Test Cases." [Online]. Available: <https://electricgrids.engr.tamu.edu/electric-grid-test-cases/>.
- [5] "EPRI | Smart Grid Resource Center > Simulation Tool – OpenDSS." [Online]. Available: <https://smartgrid.epri.com/SimulationTool.aspx>.
- [6] "The basics of primary distribution circuits," *Electrical Engineering Portal*, 28-Aug-2017. [Online]. Available: <https://electrical-engineering-portal.com/primary-distribution-circuits>.
- [7] K. P. Schneider, Y. Chen, D. Engle, and D. Chassin, "A Taxonomy of North American radial distribution feeders," in *2009 IEEE Power Energy Society General Meeting*, 2009, pp. 1–6.
- [8] "ARPA-E | GRID DATA." [Online]. Available: <https://arpa-e.energy.gov/?q=arpa-e-programs/grid-data>.
- [9] "SMART-DS: Synthetic Models for Advanced, Realistic Testing: Distribution Systems and Scenarios." [Online]. Available: <https://www.nrel.gov/grid/smart-ds.html>.
- [10] S. S. Saha, E. Schweitzer, A. Scaglione, and N. G. Johnson, "A Framework for Generating Synthetic Distribution Feeders using OpenStreetMap," *ArXiv191007673 Cs Eess*, Oct. 2019.
- [11] C. Mateo Domingo, T. Gomez San Roman, A. Sanchez-Miralles, J. P. Peco Gonzalez, and A. Candela Martinez, "A Reference Network Model for Large-Scale Distribution Planning With Automatic Street Map Generation," *IEEE Trans. Power Syst.*, vol. 26, no. 1, pp. 190–197, Feb. 2011.
- [12] A. B. Birchfield, T. Xu, K. M. Gegner, K. S. Shetye, and T. J. Overbye, "Grid Structural Characteristics as Validation Criteria for Synthetic Networks," *IEEE Trans. Power Syst.*, vol. 32, no. 4, pp. 3258–3265, Jul. 2017.
- [13] A. B. Birchfield *et al.*, "A Metric-Based Validation Process to Assess the Realism of Synthetic Power Grids," *Energies*, vol. 10, no. 8, p. 1233, Aug. 2017.
- [14] E. Schweitzer, A. Scaglione, A. Monti, and G. A. Pagani, "Automated Generation Algorithm for Synthetic Medium Voltage Radial Distribution Systems," *IEEE J. Emerg. Sel. Top. Circuits Syst.*, vol. 7, no. 2, pp. 271–284, Jun. 2017.
- [15] T. N. Kipf and M. Welling, "Semi-Supervised Classification with Graph Convolutional Networks," *ArXiv160902907 Cs Stat*, Feb. 2017.
- [16] S. Fan and B. Huang, "Labeled Graph Generative Adversarial Networks," *ArXiv190603220 Cs Stat*, Jun. 2019.
- [17] J. You, R. Ying, X. Ren, W. L. Hamilton, and J. Leskovec, "GraphRNN: Generating Realistic Graphs with Deep Auto-regressive Models," *ArXiv180208773 Cs*, Jun. 2018.
- [18] B. Xu, N. Wang, T. Chen, and M. Li, "Empirical Evaluation of Rectified Activations in Convolutional Network," *ArXiv150500853 Cs Stat*, Nov. 2015.
- [19] Z. Qin and D. Kim, "Rethinking Softmax with Cross-Entropy: Neural Network Classifier as Mutual Information Estimator," *ArXiv191110688 Cs Stat*, Jan. 2020.
- [20] I. Goodfellow *et al.*, "Generative Adversarial Nets," in *Advances in Neural Information Processing Systems* 27, 2014, pp. 2672–2680.
- [21] M. Arjovsky, S. Chintala, and L. Bottou, "Wasserstein GAN," *ArXiv170107875 Cs Stat*, Dec. 2017.
- [22] S. Ruder, "An overview of gradient descent optimization algorithms," *ArXiv160904747 Cs*, Jun. 2017.
- [23] H. Thanh-Tung and T. Tran, "On Catastrophic Forgetting and Mode Collapse in Generative Adversarial Networks," *ArXiv180704015 Cs Stat*, Oct. 2019.